# Analysis of a fractional system composed of an I-element and a fractance

Xavier Moreau, Pascal Serrier, Rachid R. Malti, Firas Khemane

# ANALYSIS OF A FRACTIONAL SYSTEM COMPOSED OF AN *I*-ELEMENT AND A FRACTANCE

**Xavier MOREAU, Pascal SERRIER,**
**Rachid MALTI and Firas KHEMANE**

*Bordeaux University - IMS, 351 cours de la Libération,*
*33 405 Talence Cedex, France*
*{firstname.name}@ims-bordeaux.fr*

Abstract: This paper deals with a fractional system composed of a storage *I*-element and a fractance. The fractance is approximate by a network of 4 identical *RC* cells arranged in gamma and a purely capacitive cell, thus defining a rational system. When compared to each other, the dynamic behaviors of the fractional and the rational system show an excellent superposition of frequency and time-domain responses. Moreover, the robustness of stability margins obtained with both systems is illustrated versus variations of the *I*-element. *Copyright © 2008 IFAC*

Keywords: fractional system, robustness, dynamic behavior, initial conditions.

## 1. INTRODUCTION

The port-based approach (as represented in a bond-graph) has demonstrated the benefits of using an integral causal form of the constitutive relations of storage ports, both for numerical simulation and the modelling process itself. In numerical simulation, integration is preferred to differentiation for obvious reasons like numerical noise and proper handling of initial conditions. For example, with a storage *C*-element (using bond-graph terminology stands for: springs, torsion bars, electrical capacitors, gravity tanks, accumulators, …) (Dauphin-Tanguy, 2000), the causal relation between the power variables is given by:

$$e_C(t) = \frac{1}{c}\int_0^t f_C(\tau)\,d\tau + e_C(0)\ , \qquad (1)$$

where $f_C(t)$ and $e_C(t)$ are the generalized flow and the generalized effort, $e_C(0)$ being an initial condition (I.C.) on the effort and $c$ a characteristic parameter of the *C*-element. With a storage *I*-element (using bond-graph terminology stands for: mass in translation, inertia in rotation, electrical or hydraulic self inductance, …), the causal relation between the power variables is given by:

$$f_I(t) = \frac{1}{l}\int_0^t e_I(\tau)\,d\tau + f_I(0)\ , \qquad (2)$$

where $f_I(t)$ and $e_I(t)$ are the generalized flow and the generalized effort, $f_I(0)$ being an initial condition on the flow and $l$ a characteristic parameter of the *I*-element.
Figure 1 presents two block diagrams that illustrate the causal relations for the *C*-element and *I*-element.

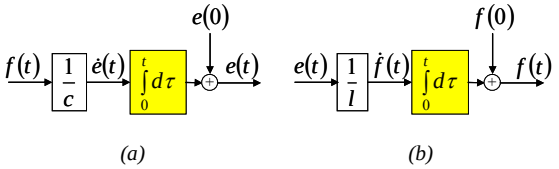


Fig. 1. Block diagrams of the *C*-element (a) and *I*-element (b)

For fractional systems, the benefits of using integral causal form are the same as rational systems (Trigeassou, *et al.,* 1999).

In this paper, the fractional system studied is composed of a storage *I*-element and a fractance defined by (Le Méhauté, *et al.,* 1998). For the fractance, the generalized effort $e_\lambda(t)$ is proportional to the fractional integral of the generalized flow $f_\lambda(t)$, namely:

$$e_\lambda(t) = \frac{1}{\lambda} \int_0^t \frac{1}{\Gamma(1-m)\,(t-\tau)^{-m}}\; f_\lambda(\tau)\; d\tau + e_\lambda(0), \qquad (3)$$

where $e_\lambda(0)$ is a function that takes into account the initial conditions (Hartley and Lorenzo, 2002; Hartley and Lorenzo, 2007; Lorenzo and Hartley, 2007a,b) and where $\lambda \in R^+$ and $m \in [0\,,1]$ ; if $m$ = 0 then the fractance is a purely capacitive *C*-element, if $m$ = 1 then the fractance is a purely resistive *R*-element.

The objective of this paper is:
- firstly, to compare the dynamic behaviors obtained with the fractance and with an approximation by a network of *N* identical *RC* cells, in particular when *N* is small (for example *N* = 4);
- then, to highlight the damping robustness versus variation of the *I*-element.

After this brief introduction, part 2 presents the modeling of the fractional system studied in this paper. Part 3 focuses on the analysis of the forced motion and part 4 on the free motion. Finally, conclusions are given in part 5.

## 2. FRACTIONAL DYNAMIC SYSTEM

In order to be generic, the relation (3) is rewritten under the form of a convolution product, namely:

$$e_\lambda(t) = g(t) * f_\lambda(t) + e_\lambda(0), \qquad (4)$$

where $g(t)$ is the impulse response $h(t)$ of the fractance or $\tilde{h}(t)$ that of its approximation.

This study being generic, no domain is privileged. However, in order to facilitate the representation, "electric diagrams" are used.

Figure 2 presents the diagram of the studied fractional system where $e_0(t)$ is a generalized effort generator and $f(t)$ the generalized flow of the *I*-element. More precisely, the diagram of figure 2.a presents the association of the *I*-element with the fractance and the diagram of figure 2.b that of the *I*-element with the approximation of the fractance.

The approximation is a cascaded network of 4 identical *RC* cells arranged in gamma, except the cell number 0 which is purely capacitive. The role of the capacitance $C_0$ is essential in the achievement of a fractional integrator with a limited number *N* of cells. All the details of this network are given in (Moreau, *et al.,* 2008).

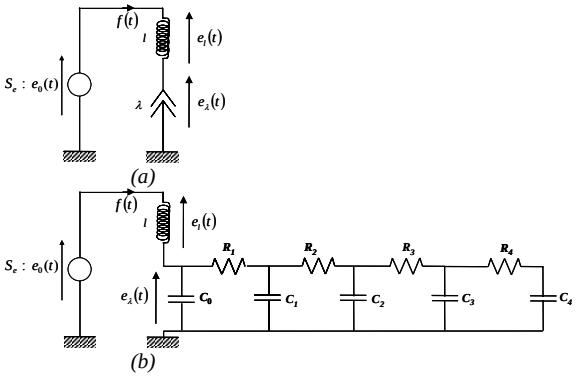


Fig. 2. Electric circuits composed of an *I*-element with a fractance (a) and an *I*-element with an approximation of this fractance (b)

The *I*-element and the fractance being in series, the generalized flow $f(t)$ through each element is the same. Hence, the generalized effort $e_0(t)$ is equal to the sum of $e_I(t)$ and $e_\lambda(t)$, namely:

$$e_0(t) = e_I(t) + e_\lambda(t). \qquad (5)$$

Finally, the causal relations of the system are:

$$\begin{cases} e_I(t) = e_0(t) - e_\lambda(t) \\ f(t) = \dfrac{1}{I} \int_0^t e_I(\tau)\, d\tau + f(0) \\ e_\lambda(t) = g(t) * f(t) + e_\lambda(0) \end{cases} . \qquad (6)$$

Figure 3 presents a causal diagram established from relations (6) and used for numerical simulations.

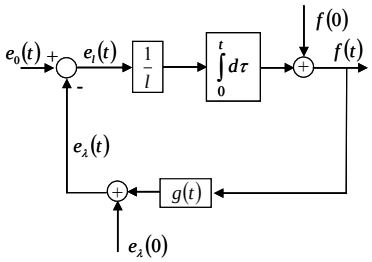


Fig. 3. Causal diagram used for numerical simulations

Such diagram presents a closed-loop structure. Relations between open-loop and closed-loop are used for analysis purposes in following paragraph. Moreover, the system being linear, the superposition principle is applied to study forced response $(e_0(t) \neq 0 \text{ and I.C.} = 0)$, then free response $(e_0(t) = 0 \text{ and I.C.} \neq 0)$.

## 3. FORCED RESPONSE

By supposing the initial conditions equal to zero, the Laplace transform of relations (6), namely:

$$\begin{cases} E_I(s) = E_0(s) - E_\lambda(s) \\ F(s) = \dfrac{1}{I\,s}\, E_I(s) \\ E_\lambda(s) = G(s)\; F(s) \end{cases} , \qquad (7)$$

allows to establish the functional diagram of figure 4 presents where $\beta(s)$ is the open-loop transfer function given by:

$$\beta(s) = G(s)\frac{1}{l\,s}\ , \qquad (8)$$

with

$$G(s) = H(s) = \frac{1}{\lambda\ s^{1-m}} \qquad (9)$$

for the fractance, and

$$G(s) = \tilde{H}(s) = \frac{D_0}{s}\left(\frac{1+\sum_{i=1}^{N=4} b_i\,(RC\,s)^i}{1+\sum_{i=1}^{N=4} a_i\,(RC\,s)^i}\right) \qquad (10)$$

for its approximation (Moreau, *et al.*, 2008).

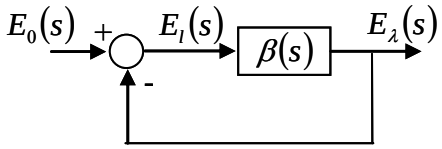


Fig. 4. Functional diagram for analysis

In the case of the fractance, the expression of $\beta(s)$ is:

$$\beta(s) = \frac{b}{s^n}\ , \qquad (11)$$

where $n = 2 - m$ and $b = 1/(l\lambda)$. The closed-loop transfer is given by

$$T(s) = \frac{E_\lambda(s)}{E_0(s)} = \frac{b}{s^n + b}\ . \qquad (12)$$

Figure 5 presents the responses of the fractional system obtained with the fractance (——) and its approximation (- - - -) for the nominal value $l_0$ of the parameter $l$. More precisely, the frequency responses of the fractional integrator and its approximation are presented in figure 5.a; the open-loop Nichols loci in figure 5.b ; the gain diagrams of the closed-loop transfer in figure 5.c and the step responses of $e_\lambda(t)$ to an unit step $e_0(t)$ in figure 5.d.

It is important to note the excellent superposition of the frequency responses (figure 5.c) and of the step responses (figure 5.d) of the closed-loop obtained with the fractional integrator and its approximation. This result is very interesting as far as the fractional behavior is only synthesized in a single decade (figure 5.a). In fact, it is fundamental that the open-loop cross-over frequency $\omega_u$ belongs to this decade to obtain such a result (figure 5.b).

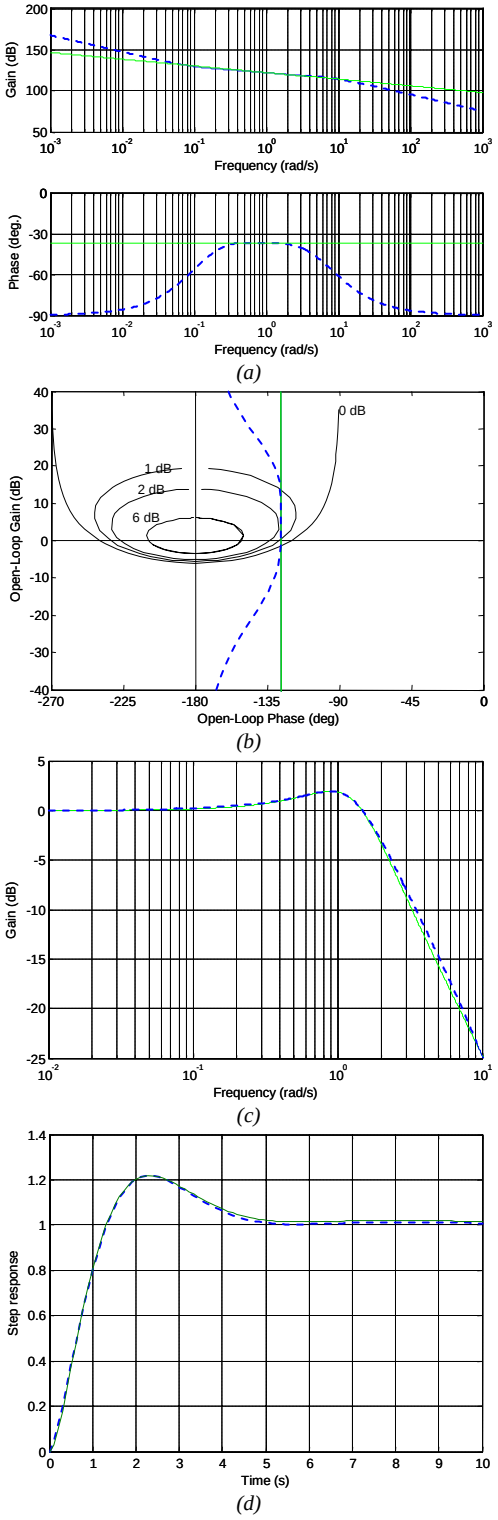


Fig. 5. Comparison of fractional system responses obtained with the fractance (——) and its approximation (- - - -): frequency responses of the fractional integrator and its approximation (a); open-loop Nichols loci (b); gain diagrams of the closed-loop transfer (c) and step responses of $e_\lambda(t)$ to an unit step $e_0(t)$ (d)

**Remark**

In a general way, the numerical simulation of frequency responses of a fractional system is not a problem. But, the numerical simulation of time responses is more delicate. So, the response $e_\lambda(t)$ to an unit step $u(t)$ (figure 5.d) is obtained firstly from its Laplace transform

$$E_\lambda(s) = T(s)\frac{1}{s} = \frac{b}{s\left(s^n + b\right)} \qquad (13)$$

and after a decomposition under the form

$$E_\lambda(s) = \frac{1}{s} - \frac{s^n}{s\left(s^n + b\right)}, \qquad (14)$$

then by the inverse Laplace transform of (14), namely:

$$e_\lambda(t) = \mathrm{TL}^{-1}\left\{\frac{1}{s} - \frac{s^n}{s\left(s^n + b\right)}\right\} = u(t) - E_n\left[-b\,t^n\right], \qquad (15)$$

where $E_n[-b\ t^n]$ is the Mittag-Leffler function (Hartley and Lorenzo, 2002) defined by

$$E_n\left[-b\,t^n\right] = \sum_{i=0}^{\infty} \frac{(-b)^i\ t^{in}}{\Gamma(in+1)}. \qquad (16)$$

So, the step response presented in figure 5.d is obtained by programming the relation (16) where the sum is truncated at $i = 100$. This value is chosen very large in order to obtain a fractional system response very close to the true one.

Considering the excellent capability that has the network of 4 identical *RC* cells arranged in gamma to reproduce the behavior of the fractance associated with an *I*-element, the next paragraph focuses on the performance obtained with this approximation.

Moreover, the parameter $l$ of the *I*-element is considered as uncertain $\left(l \in \left[l_{\min}\ ;\ l_{\max}\right]\right)$.

Figure 6 illustrates the influence of the $l$ variation on the dynamic behavior of the fractional system. More precisely, figure 6.a presents the open-loop Nichols loci, figure 6.b the gain diagrams of the closed-loop transfer and figure 6.c the step responses of $e_\lambda(t)$.

The variation of $l$ leads to an open-loop gain variation that is why the open-loop frequency responses are tangent to the same Nichols magnitude contour (figure 6.a). So, one can observe the robustness of the resonant peak (figure 6.b) and the robustness of the first overshoot (figure 6.c) versus $l$ variation.

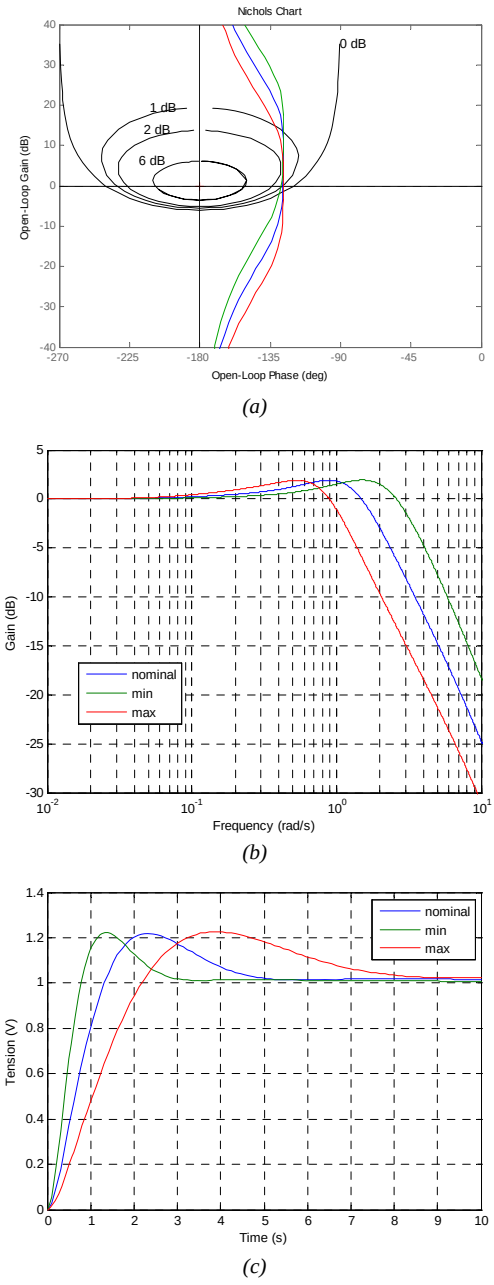


Fig. 6. Illustration of the stability margin robustness versus $l$ variation ($l_0$ blue, $l_{min}$ green and $l_{max}$ red): open-loop Nichols-loci (a); gain diagrams of the closed-loop transfer function (b) and step responses of generalized effort $e_\lambda(t)$ (c)

## 4. FREE RESPONSE

In order to facilitate the analysis of the free response, a state space representation of the fractance approximation is used, namely:

$$\begin{cases} \dot{\underline{x}} = A\,\underline{x} + B\,u \\ y = C\,\underline{x} + D\,u \end{cases}, \qquad (17)$$

where

$$u = f(t)\ ,\quad \underline{x} = \begin{pmatrix} x_1 = e_\lambda(t) \\ x_2 = e_{C1}(t) \\ x_3 = e_{C2}(t) \\ x_4 = e_{C3}(t) \\ x_5 = e_{C4}(t) \end{pmatrix}\ ,\quad y = e_\lambda(t)\ , \quad (18)$$

the $e_{Ci}(t)$ being the generalized efforts of elements $C_i$, and

$$A = \begin{bmatrix} -1/R_1C_0 & 1/R_1C_0 & 0 & 0 & 0 \\ 1/R_1C_1 & \frac{-1}{C_1}\left(\frac{R_1+R_2}{R_1R_2}\right) & 1/R_2C_1 & 0 & 0 \\ 0 & 1/R_2C_2 & \frac{-1}{C_2}\left(\frac{R_2+R_3}{R_2R_3}\right) & 1/R_3C_2 & 0 \\ 0 & 0 & 1/R_3C_3 & \frac{-1}{C_3}\left(\frac{R_3+R_4}{R_3R_4}\right) & 1/R_4C_3 \\ 0 & 0 & 0 & 1/R_4C_4 & -1/R_4C_4 \end{bmatrix}, \quad (19)$$

$$B = \begin{bmatrix} 1/C_0 \\ 0 \\ 0 \\ 0 \\ 0 \end{bmatrix},\ C = \begin{bmatrix} 1 & 0 & 0 & 0 & 0 \end{bmatrix},\ D = 0\ . \quad (20)$$

The Laplace transform of relation (17) leads to

$$\underset{(1x1)}{Y} = \underset{(1x5)}{\left(C\left[sI - A\right]^{-1}\right)}\ \underset{(5x1)}{\underline{x}(0)} + \underset{(1x1)}{\left(C\left[sI - A\right]^{-1}B\right)}\ \underset{(1x1)}{U}\ , \quad (21)$$

where $\underline{x}(0)$ is the initial condition vector associated with elements $C_i$. The relation (21) can be rewritten under the form

$$Y = \sum_{i=1}^{5}\left(\Psi_i(s)\, x_i(0)\right) + \tilde{H}(s)\, U\ , \quad (22)$$

where

$$\Psi_i(s) = \left(C\left[sI - A\right]^{-1}\right) \text{ and } \tilde{H}(s) = \left(C\left[sI - A\right]^{-1}B\right), \quad (23)$$

Finally, back to the time-domain by inverse Laplace transform leads to

$$e_\lambda(t) = \sum_{i=1}^{5}\left(TL^{-1}\{\Psi_i(s)\ x_i(0)\}\right) + \tilde{h}(t) * f(t), \quad (24)$$

relation of the form

$$e_\lambda(t) = e_\lambda(0) + \tilde{e}_\lambda(t)\ , \quad (25)$$

by putting

$$e_\lambda(0) = \sum_{i=1}^{5}\left(TL^{-1}\{\Psi_i(s)\ x_i(0)\}\right) \quad (26)$$

and

$$\tilde{e}_\lambda(t) = \tilde{h}(t) * f(t)\ . \quad (27)$$

So, the functional diagram of figure 3 is completed in accordance with previous developments (figure 7).

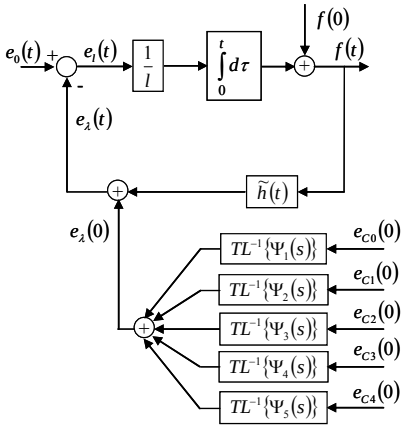


Fig. 7. Functional diagram for simulation by taking into account the initial conditions $e_{Ci}(0)$ associated with elements $C_i$

For the study of free response $e_0(t) = 0$, and the initial conditions are:

$$f(0) = 0 \quad \text{and} \quad e_{Ci}(0) = 1 \quad \forall\, i \in [0\,;4]\,. \quad (28)$$

In this case and for the nominal value $l_0$ of the parameter $l$, figure 8.a presents the contributions of each term of the sum $e_\lambda(0)$ defined by the relation (26). Figure 8.b shows the plot of $e_\lambda(0)$ (green) and the plots of $\tilde{e}_\lambda(t)$ (red) and $e_\lambda(t)$ (blue).

It is important to note that the sum $e_\lambda(0)$ of all contributions $e_{Ci}(0)$ is equal to unity.

Finally, figure 9 presents free response of $e_\lambda(t)$ for the same initial conditions and for the values $l_0$, $l_{min}$ and $l_{max}$ of $l$, showing thus the robustness of the stability margin versus $l$ variation.

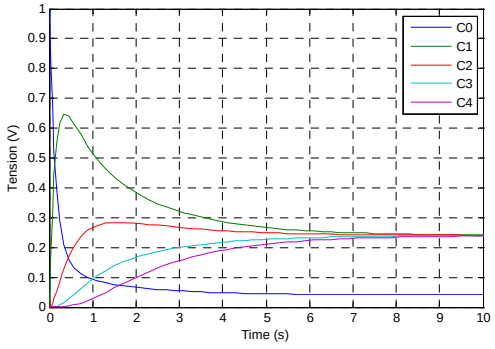


*(a)*

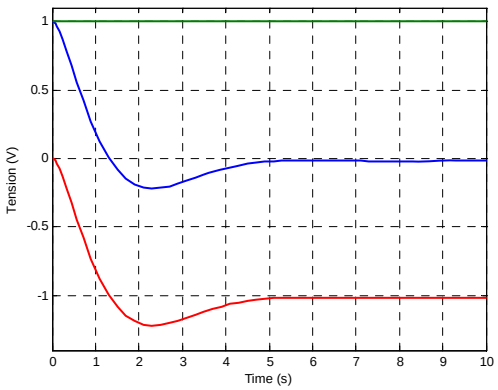


*(b)*

Fig. 8. Contributions of each term of the sum $e_\lambda(0)$ defined by the relation (26) (a) and plots of $e_\lambda(0)$ (green), $\tilde{e}_\lambda(t)$ (red) and $e_\lambda(t)$ (blue) (b)

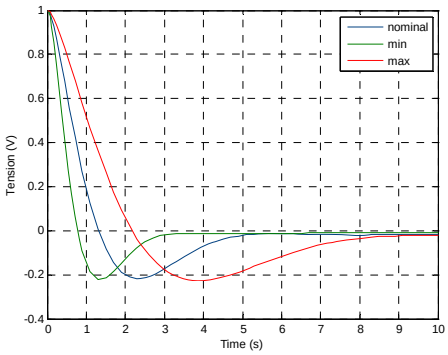


Fig. 9. Free response of $e_\lambda(t)$ for the same initial conditions and for the values $l_0$, $l_{min}$ and $l_{max}$ of $l$

In a first step, the interest of using the fractance approximation for taking into account initial conditions is to observe (in this particular case) that $e_\lambda(0)$ is equal to a constant (unity if all the $e_{Ci}(0) = 1$ and if $f(0) = 0$). In a second step, it is possible to affirm (always in this particular case) that $e_\lambda(0)$ is an unit constant and to replace the impulse response $\tilde{h}(t)$ of the approximation by that of the fractance, namely $h(t)$. Thus, with $e_0(t) = 0$, $f(0) = 0$ and $e_\lambda(0) = 1$, the relation (6) is rewritten under the form:

$$\begin{cases} e_l(t) = -e_\lambda(t) \\ f(t) = \dfrac{1}{l}\int_0^t e_l(\tau)\,d\tau \\ e_\lambda(t) = h(t) * f(t) + e_\lambda(0) \end{cases}, \qquad (29)$$

where $$h(t) = \frac{t^{-m}}{\lambda\,\Gamma(1-m)} \quad . \qquad (30)$$

The Laplace transform of relation (29), namely:

$$\begin{cases} E_l(s) = -E_\lambda(s) \\ F(s) = \dfrac{1}{l\,s}E_l(s) \\ E_\lambda(s) = \dfrac{1}{\lambda\,s^{1-m}}F(s) + \dfrac{e_\lambda(0)}{s} \end{cases}, \qquad (31)$$

leads to an expression of the form

$$E_\lambda(s) = -\frac{1}{\lambda\,s^{1-m}}\frac{1}{l\,s}E_\lambda(s) + \frac{e_\lambda(0)}{s}, \qquad (32)$$

that can be reduced to

$$E_\lambda(s) = \frac{s^n}{s\left(s^n + b\right)}e_\lambda(0), \qquad (33)$$

always by putting $n = 2 - m$ and $b = 1/(l\lambda)$. Knowing that $e_\lambda(0) = 1$, the inverse Laplace transform leads to:

$$e_\lambda(t) = \mathrm{TL}^{-1}\left\{\frac{s^n}{s\left(s^n + b\right)}\right\} = E_n\left[-b\,t^n\right], \qquad (34)$$

where $E_n[-b\,t^n]$ is the Mittag-Leffler function defined by the relation (16).

Figure 10 presents, for the nominal value $l_0$, the free motion of $e_\lambda(t)$ obtained with the approximation (- - - -) and with the Mittag-Leffler function (——) truncated at $i = 100$. One can observe the excellent superposition of the two plots.

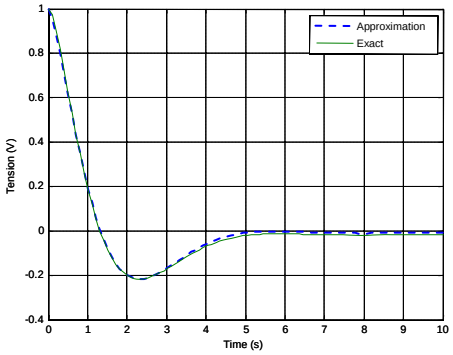


Fig. 10. Free response of $e_\lambda(t)$ obtained with the approximation (- - - -) and with the Mittag-Leffler function (——) truncated at $i = 100$

## 5. CONCLUSION

In this paper, a fractional system and its approximation have been studied. The comparison of the dynamic behaviors obtained with both systems shows the excellent capability that has the network of 4 identical *RC* cells arranged in gamma to reproduce the behavior of the fractance. Moreover, the robustness of stability margin obtained with both systems is illustrated versus the *I*-element variation.
The perspectives in the continuity of this study are a take into account uncertainties and/or non-linearities of the *R* and *C* elements according to context of the application.

## REFERENCES

Dauphin-Tanguy G. (2000). Les bond-graphs, Edition Hermès, Paris.

Hartley T.T. and C.F. Lorenzo (2002). Dynamics and Control of Initialized Fractional-Order Systems. *Journal of Nonlinear Dynamics*, Vol. 29, pp. 201-233, Kluwer Academic Publishers.

Hartley T.T. and C.F. Lorenzo (2007). Application of incomplete gamma functions to the initialization of fractional-order systems. *Proceedings of the ASME 2007*, DETC2007-35843, Las Vegas, Nevada, USA, September 4-7.

Le Méhauté A., R. Nigmatullin et L. Nivanen (1998). Flêche du temps et géométrie fractale, Edition Hermès, Paris.

Lorenzo C.F. and T.T. Hartley (2007a). Initialization of fractional differential equations: background and theory. *Proceedings of the ASME 2007*, DETC2007-34810, Las Vegas, Nevada, USA, September 4-7.

Lorenzo C.F. and T.T. Hartley (2007b). Initialization of fractional differential equations: theory and application. *Proceedings of the ASME 2007*, DETC2007-34814, Las Vegas, Nevada, USA, September 4-7.

Moreau X., P. Serrier and A. Oustaloup (2008). From fractional systems to localised parameter systems: synthesis and analysis. *Special Issue on APII-JESA*, N° 6-7-8, volume 42, September.

Trigeassou J.C., T. Poinot, J. Lin, A. Oustaloup, F. Levron (1999). Modeling and identification of a non integer order system. *Proceedings of ECC'99*, European Control Conference, Karlsruhe, Germany.